Mineralogical Magazine, August 1999, Vol. 63(4), pp. 567–578

Fresh and weathered pyrochlore studies by Fourier transform infrared spectroscopy coupled with thermal analysis

M. Nasraoui*, E. Bilal and R. Gibert

Département de Géochimie, Ecole des Mines de Saint Etienne, 158, Cours Fauriel 42023, Saint Etienne Cedex 02, France

ABSTRACT

Fresh and weathered pyrochlore from the Lueshe carbonatite complex (in the northeast of the Democratic Republic of Congo) was studied by Fourier transfom infrared (FTIR) spectroscopy and by a combination of FTIR spectroscopy and thermal analysis. The former was carried out in the spectral range 400–4000 cm^{-1}. The spectra for fresh and weathered pyrochlores were very different. For the weathered pyrochlore, two bands were identified as OH vibration modes, one broad band with a maximum at 3413 cm^{-1} and another finer band at 1630 cm^{-1}. The fresh pyrochlore does not show OH absorption bands. The presence of OH confirms the hydrated state of the weathered pyrochlore suggested by previous microanalytical work. The combination of FTIR spectroscopy and thermal analysis allows 'real-time' observation of gas emanations and solid-state transformations taking place during heating up to 800°C. For fresh pyrochlore, no solid transformation was detected, except a CO_2 emanation from 242–576°C. For the weathered pyrochlore a dehydration was observed between 234–565°C followed by an exothermic peak in Differential Scanning Calorimetric (DSC) curve at 604°C. This exothermic peak corresponds to the formation of a Nb oxide phase. At higher temperatures the weathered pyrochlore is partly decomposed, forming a dehydrated pyrochlore and a Nb oxide phase. The combination of FTIR and thermal analysis has provided useful information on both fresh and weathered pyrochlore transformations which has clarified our understanding of the water control of the structural stability of pyrochlore minerals.

Keywords: pyrochlore, weathering, IR spectroscopy, heating, solid state transformations.

Introduction

Earlier research concerning pyrochlore of the Lueshe ore deposit has identified different chemical transformations affecting this mineral during laterization processes (Van Wambeke, 1978; Albers *et al.*, 1994; Philippo, 1995; Nasraoui, 1996; Wall *et al.*, 1996). Wall *et al.* (1996) and Nasraoui (1996) have studied the chemical variations of pyrochlore belonging to both the carbonatites and the laterite. These authors reported that the pyrochlore from the fresh rocks (carbonatites) presents a structural formula close to the ideal formula: $(Ca,Na)_2Nb_2O_6(OH,F)$, whereas the structural formula of the weathered pyrochlore from the laterite corresponds to $A_{2-x}B_2O_6(OH,F)_{1-y}4{\cdot}zH_2O$ which seems to result from intense leaching and partial exchange of *A* cations. The chemical compositions of weathered pyrochlore have lower totals than those of fresh pyrochlores. According to the authors mentioned above, such a deficit could be explained by extensive hydration of weathered pyrochlore. This corroborates the results of Ercit *et al.* (1994) on the refinement of the structure of the kalipyrochlore of Lueshe. The following empirical structural formula was suggested for weathered pyrochlore: $([H_2O]_{0.99}Sr_{0.05}Ca_{0.01})_{\Sigma 1.05}(Nb_{1.80}Ti_{0.20})_{\Sigma 2.00}(O_{4.06}OH_{1.94})_{\Sigma 6.00}([H_2O]_{0.86}K_{0.14})_{\Sigma 1.00}$.

The current investigation, which complements chemical data obtained using microprobe

---

* Present address: Instituto Technologico e Nuclear, EN10, 2686-953, Sacavém, Portugal

analysis, provides a comparative study between fresh and weathered pyrochlore of the lateritic Nb deposit of Lueshe using FTIR spectroscopy and a combination of FTIR and thermal analysis. The aim is to confirm the hydration state of pyrochlore during weathering processes, as well as to describe and interpret the role of water in the stability of these minerals. To our knowledge, no study combining FTIR and thermal analysis has previously been carried out on pyrochlore.

Geological framework

The plutonic complex of the Lueshe syenite/carbonatite is located in the northeast of the Democratic Republic of Congo at 29°7′E and 0°59′S in the Rwindi Mountains (De Bethune, 1949), ~40 km southwest of Lake Edward (Idi Amin) and 70 km north of Lake Kivu. The Lueshe complex forms a part of the anorogenic plutonic and plutovolcanic alkaline complexes of the vast lake district which is bounded by Lake Albert (Mobutu) to the north and Lake Tanganyika to the south. These carbonatite complexes are located along the western branch of the East African rift (De Bethune, 1952; Lubala *et al.*, 1985). The K/Ar age of a biotite from a sövite is 516 ± 26 Ma (Bellon and Pouclet, 1980). The geological framework of the Lueshe complex was described by Meyer (1958), Maravic and Morteani (1980) and Maravic *et al.* (1989). This complex is an alkaline plutonic massif with a sub-elliptical shape extending ~3 km NW–SE and 2 km NE–SW. It intrudes the metamorphic host series, consisting of micaschists, quartzites and amphibolites of Burundian age (1100 Ma). It consists of a central core of cancrinite syenite and alkaline-feldspar syenite, bordered by a calcite carbonatite ring. The outcrop of dolomite carbonatite is limited to the SE part of the complex. Sodic and potassic fenitizations of variable intensities were also observed at some contacts between carbonatite and the host rock (Van Overbeke, 1996).

At Lueshe, after a limited hydrothermal alteration (Nasraoui, 1996), a long ferrallitic period produced an important laterite cover in the southern half of the complex (30–150 m thick). Weathering of the fresh rocks consisted of a decarbonatization correlated with a high volume reduction and a relative enrichment of the content of resistant primary minerals (apatite, feldspar, pyrochlore and zircon). Subsequently, the intensification of the alteration ended with the dissolution of the apatite and a significant increase in the amount of secondary minerals, such as an aluminous phosphate of the crandallite group, clay minerals of the kaolinite group and iron oxides. At this alteration stage small amounts of Mn oxide, rhabdophane-(Ce), wavellite, variscite and jarosite were also found.

The order and the nature of these weathering transformations induce a significant enrichment of pyrochlore in the lateritic profile. Pyrochlore is most abundant in the upper, more highly weathered ore concentrations and has undergone numerous chemical transformations.

Material and analytical procedure

Fourier transform infrared spectroscopy

A FTIR spectroscopy study was carried out on a fresh pyrochlore from the sövite and on a weathered pyrochlore from the laterite. The pyrochlore grains were obtained by electromagnetic and heavy-liquid separation, followed by separation under a binocular microscope. The level of purity of the separated grains was checked by X-ray diffraction (XRD) (Siemens Diffractometer D 5000), and by scanning electron microscopy (SEM) (JEOL JSM80).

The IR equipment used in absorption mode is a Digilab FTS 185, in a spectral domain from 4000 to 400 cm^{-1}. The grains were crushed to a size of <2.5 μm as observed under the SEM. Due to the high absorption intensity, the crushed samples were diluted in potassium bromide (KBr) which is inactive in the wavelength range used. For dilution, 10 mg (with an accuracy of 10^{-4} g) of crushed material were weighed together with 600 mg of KBr (crushed and dried at 110°C). Then, 150 mg of the mixture sample-KBr were pressed, after homogenization in a steel mould, for 2 min at a pressure of 10 tonnes. The IR spectra represent an average of 32 scans between 4000 and 400 cm^{-1} with a resolution of 4 cm^{-1}. The reproducibility of the data was monitored by several determinations on the same sample. The treatment and presentation of the spectra were achieved using the GRAMS software.

Fourier transform infrared spectroscopy coupled with thermal analysis

The equipment used for the IR analysis of gas is a Digilab FTS 40 equipped with a gas compartment where the thermostatic cell has a length of 10 cm. This gas compartment is permanently swept by the gas issued from the thermal analyser. The thermal analyser is a Setaram DSC 111 allowing thermogravimetric analysis, as well as enthalpy measurements. The operating conditions for gas analysis by IR are four scans with a resolution of 8 cm^{-1}, the spectral domain extending from 4000 to 700 cm^{-1}. The transfer line was brought by thermostat to 150°C and the thermostatic cell to 180°C. Appropriate software was used, allowing permanent acquisition of spectra (~1 spectrum s^{-1}). A stepwise increase of 20°C/min was used in order to detect the enthalpy variations. However, more precise measurements needed a slower rate of temperature increase (10°C/min), in order to ensure an equilibrated thermal balance in the sample. It should to be pointed out that the protective quartz layers for the calorimetric analyses have a delay effect on the precise temperature of the process (delayed thermal transfer). The increase in temperature was carried out from room temperature to 800°C, argon being the the flowing gas used.

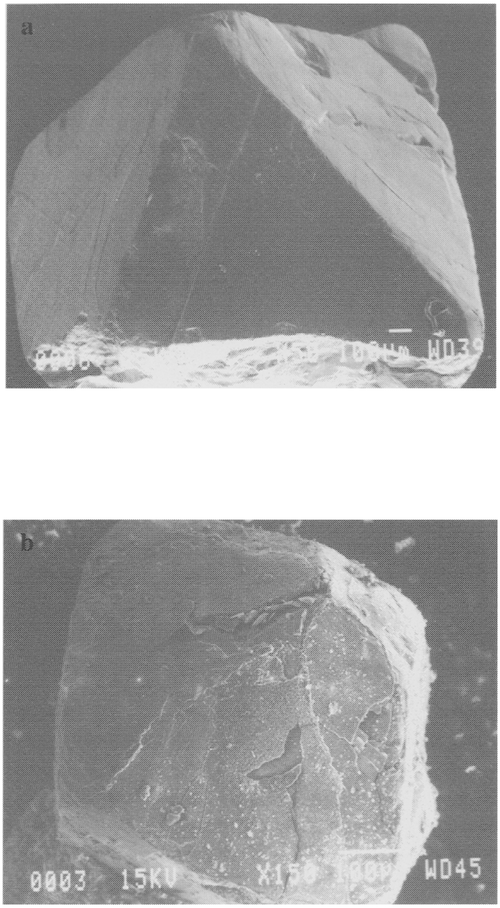

FIG. 1. SEM images (secondary electron) of pyrochlore from Lueshe: (*a*) fresh, euhedral pyrochlore; (*b*) weathered pyrochlore.

Mode of occurrence of pyrochlore

Pyrochlore in the carbonatite

The minerals of the pyrochlore group show a variety of chemical compositions. The general structural formula can be written as $A_{2-m}B_2X_{6-w}Y_{1-n}pH_2O$ (Hogarth, 1977; Lumpkin, 1989; Lumpkin *et al.*, 1986). The octa-coordinated *A* site can be filled by Na, Ca, Mn, Fe^{2+}, Sr, Sb, Cs, Ba, *REE*, Pb, Bi, Th or U. The hexacoordinated *B* site can be filled by Nb, Ta, Ti, Al, Fe^{3+}, Zr, Sn or W (Hogarth, 1989). The *X* site contains oxygen, or even OH ions (Ercit *et al.*, 1994). The *Y* site can contain O, F or OH.

Pyrochlore is the main magmatic Nb-mineral in the Lueshe carbonatite, containing >99.9% of the available Nb. It is present as an accessory mineral with normative values of 1% in sövite, 1–2% in the rocks of the contact zones, such as syenite, fenite and pyroxenite. The pyrochlore grains are greenish to yellowish in colour; they are subhedral to euhedral, and they range from 0.1–2 mm in diameter. (Fig. 1*a*). Pyrochlore is seldom found as inclusions in other minerals, except in some calcites and apatites in the sövites. On the other hand, pyrochlore often contains inclusions of calcite, dolomite and apatite. Microprobe analyses (Table 1) indicate that the fresh pyrochlore of the Lueshe deposit is not hydrated, with a chemical composition close to the ideal structural formula $(Ca,Na)_2Nb_2O_6(OH,F)$ (Hogarth, 1977; Lumpkin *et al.*, 1986; Lumpkin, 1989).

For fresh pyrochlore, the average value of *A*-site occupancy is 96% when calculated for 2 *B*-site cations. The *A* site is often occupied by Ca and Na with atomic variations ranging from 0.6–1.19 and from 0.74–1.21, respectively. The sum of the other ions (K, Sr, Ba, *REE*) does not exceed 3%, on average, for the total occupancy of site *A*.

The *B* site is mainly occupied by Nb with a small amount of Ti, and also by Ta (in the syenitic pyrochlore). The number of atoms varies between 1.67 and 1.91 for Nb, between 0.08 and 0.22 for

TABLE 1. Selected electron microprobe analyses of fresh and hydrothermally-altered pyrochlore

	Fresh pyrochlore			Hydrothermally altered pyrochlore		
	Sövite					
Na_2O	7.05	7.73	7.14	2.4	1.44	3.16
SiO_2	0.01	0.07	0.13	1.83	1.59	1.04
K_2O	0	0	0	0.28	0.13	0.11
CaO	13.6	13.81	13.48	8.8	9.92	11.86
TiO_2	2.93	3.29	3.28	2.93	3.5	3.3
Fe_2O_3	0.05	0.13	0.25	1.87	2.03	1.49
SrO	1.11	1.06	1.46	5.83	5.56	3.71
Y_2O_3	<dl	<dl	<dl	<dl	<dl	<dl
ZrO_2	0	0	0.02	0.02	0	0
Nb_2O_5	68.5	67.84	67.38	64.3	66.46	65.64
BaO	0.07	0	0.04	0.02	0.60	0.17
La_2O_3	0.63	0.31	0.33	1.47	0.40	0.26
Ce_2O_3	0.89	0.58	0.76	3.06	0.80	0.96
Ta_2O_5	0	0	0	0	0	0
F	4.97	5.66	4.88	1.73	2.31	2.85
Total	99.81	100.48	99.14	94.54	94.74	94.55
Structural formula calculated to 2 *B* site cations						
Na	0.823	0.900	0.833	0.270	0.156	0.357
K	0	0	0	0.021	0.009	0.008
Ca	0.877	0.888	0.869	0.546	0.594	0.741
Sr	0.025	0.024	0.033	0.127	0.117	0.081
Y	–	–	–	–	–	–
Ba	0.002	0	0.001	0	0.013	0.004
La	0.014	0.007	0.007	0.031	0.008	0.006
Ce	0.020	0.013	0.017	0.065	0.013	0.021
A site	1.761	1.832	1.759	1.060	0.914	1.217
Si	0.001	0.004	0.008	0.106	0.089	0.061
Ti	0.133	0.149	0.148	0.128	0.147	0.145
Fe	0.002	0.006	0.011	0.082	0.085	0.065
Zr	0	0	0.001	0.001	0	0
Nb	1.864	1.841	1.832	1.684	1.679	1.729
Ta	0	0	0	0	0	0
B site	2	2	2	2	2	2
Total O	6.297	6.309	6.266	5.765	5.640	5.880
F	0.946	1.075	0.928	0.317	0.408	0.525

Total Fe as Fe_2O_3; total Ce as Ce_2O_3;
<dl = below detection limit.

Ti, and between 0 and 0.04 for Ta. The SEM observations, microprobe analysis and X-ray images of the element distributions, as well as the characterizations of the mineral parageneses outline the hydrothermal alteration of pyrochlore (Nasraoui, 1996). The hydrothermal transformations of these minerals cause important changes in their compositions, most notably: (1) a leaching of Na and Ca from the *A* site and their partial replacement by Sr and light rare-earth elements (*LREE*); (2) a leaching of F from the *Y* site; and, (3) hydration.

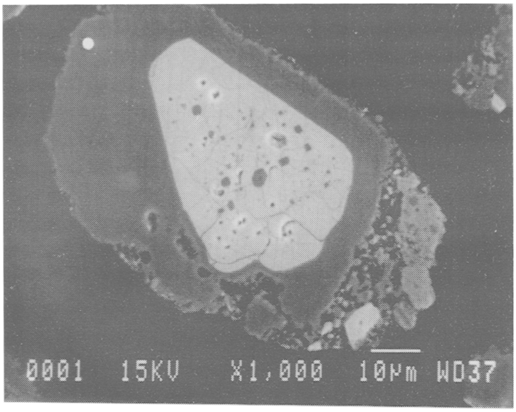

FIG. 2. SEM image (secondary electron) of weathered pyrochlore crystal with an external crandallite coating.

Pyrochlore in the laterite

Textural relationship among the neoformed phases

The supergene alteration of the Lueshe complex caused a complex mobilization and redistribution of the chemical elements. This mobilization was influenced by various factors especially by the ease of alteration of the primary phases. Pyrochlore, which is relatively resistant to supergene alteration, underwent a relative accumulation in the lateritic profile. This accumulation was accompanied by chemical and textural transformations without any change in the mineralogical state (Albers *et al.*, 1994; Nasraoui, 1996; Wall *et al.*, 1996).

The very crumbly pyrochlore grains are subhedral to euhedral and often fractured and porous (Fig. 1*b*). The solid inclusions of calcite and apatite frequently found in the fresh pyrochlores, are absent in weathered pyrochlores. The greenish colour of the fresh pyrochlore crystals becomes whitish to milky white in the lateritic facies. Weathered pyrochlores often present intergrowths of aluminous phosphate as an external coating (Fig. 2), as well as fracture and cavity fillings.

Chemical changes in the pyrochlore during weathering

From a chemical point of view, pyrochlores are very vulnerable to supergene conditions. The

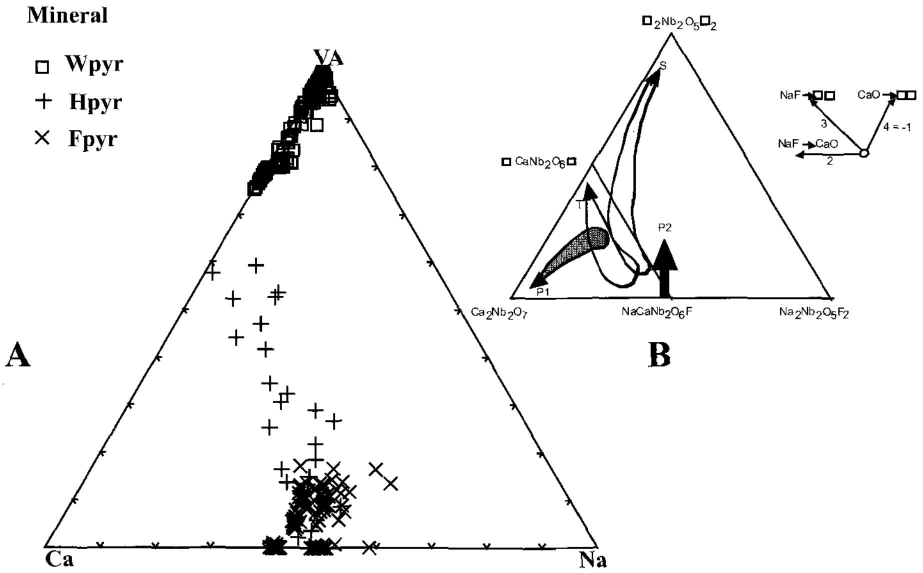

FIG. 3. Triangular plot (atomic ratios) showing the alteration trends of pyrochlore. (*A*) A plot of *VA* (*A*-site vacancies), Ca and Na of fresh pyrochlore (Fpyr) and altered pyrochlores of Lueshe. Hpyr: Hydrothermally altered pyrochlore and Wpyr: weathered pyrochlore. For comparison, we show (*B*) the results of Lumpkin and Ewing (1995). P1 = primary alteration of uranpyrochlore from granitic pegmatites, P2 = primary alteration of (Na,Ca)-pyrochlore from nepheline syenites and carbonatites, T = transitional alteration and S = secondary alteration.

TABLE 2. Selected electron microprobe analyses of weathered pyrochlores from Lueshe laterite. Ce as Ce^{4+} in ceriopyrochlore analyses, as Ce^{3+} and Ce_2O_3 in the other analyses

	Kali-pyrochlore		Low-Na pyrochlore		Strontio-pyrochlore		Cerio-pyrochlore		Bario-pyrochlore	
K_2O	4.58	1.47	0.51	0.91	1.76	0.10	2.84	1.53	0.72	1.19
Na_2O	0.28	0.04	0.03	0.21	0.12	0.07	0.26	0.19	0.54	0.15
CaO	0.13	0.09	7.96	5.20	1.70	1.04	1.28	1.44	0.26	1.36
SrO	0.68	0.66	0.48	0.57	6.60	11.86	1.32	0.30	1.24	0.86
BaO	0.21	0.31	0.52	0.23	0.24	0.02	0.16	0.43	13.62	10.09
La_2O_3	0.07	0	0.07	0.13	0	0.10	0.12	0	0	0.03
Ce_2O_3/CeO_2	0	0.05	0	0	0.89	10.68	10.63	15.41	0	0.47
Y_2O_3	0	0	0.14	0	0	0	0	0.14	0	0
Al_2O_3	0.11	0	0	0	0.02	0	1.39	0	0	0.17
SiO_2	0.18	0.06	0.40	1.06	0	0.78	0.21	0.49	0	0
P_2O_5	0.58	0	0	0	0	0.07	1.51	0	0	0
TiO_2	2.65	2.72	2.24	2.67	4.03	2.10	2.40	3.78	4.18	3.73
Fe_2O_3	3.61	0.25	1.87	0.42	0.71	0.69	4.16	1.28	0.74	1.28
ZrO_2	0	0	0	0	0.08	0	0	0	0	0.09
Nb_2O_5	75.04	83.18	77.12	75.20	76.10	67.35	63.13	70.82	73.55	72.05
Ta_2O_5	0	0	0	0	0.15	0	0	0	0	0.03
F	2.05	0	0.13	0	0	0.44	2.79	0.14	0	0
Sum	90.17	88.83	91.47	86.61	92.45	95.29	92.19	95.95	94.85	91.52
O = F	0.86	0	0.06	0	0	0.19	1.17	0.06	0	0
Total	89.31	88.83	91.41	86.61	92.45	95.11	91.02	95.89	94.85	91.52
Structural formula calculated to 2 *B* site cations										
K	0.296	0.094	0.034	0.062	0.118	0.008	0.198	0.108	0.050	0.083
Na	0.027	0.004	0.003	0.022	0.012	0.008	0.027	0.020	0.057	0.016
Ca	0.007	0.005	0.445	0.298	0.096	0.067	0.075	0.085	0.015	0.080
Sr	0.013	0.013	0.009	0.012	0.130	0.267	0.027	0.006	0.025	0.018
Ba	0.004	0.006	0.011	0.005	0.005	0.001	0.003	0.009	0.289	0.216
La	0.001	0	0.001	0.003	0	0.002	0.002	0	0	0.001
Ce	0	0.001	0	0	0.016	0.234	0.213	0.311	0	0.090
Y	0	0	0.004	0	0	0	0	0.004	0	0
A Site	0.349	0.122	0.506	0.401	0.378	0.586	0.546	0.543	0.436	0.424
Al	0.007	0	0	0	0.001	0	0.090	0	0	0.011
Si	0.009	0.003	0.021	0.057	0	0.047	0.011	0.027	0	0.002
P	0.025	0	0	0	0	0.004	0.070	0	0	0
Ti	0.101	0.103	0.088	0.107	0.157	0.095	0.099	0.157	0.170	0.153
Fe	0.138	0.009	0.073	0.017	0.028	0.031	0.171	0.053	0.030	0.053
Zr	0	0	0	0	0.002	0	0	0	0	0.024
Nb	1.720	1.885	1.818	1.819	1.807	1.824	1.560	1.764	1.800	1.779
Ta	0	0	0	0	0.002	0	0	0	0	0
B site	2.000	2.000	2.000	2.000	2.000	2.000	2.000	2.000	2.000	2.000
Oxy	4.988	5.012	5.363	5.262	5.220	5.712	5.332	5.647	5.267	5.245
F	0.329	0	0.022	0	0	0.084	0.482	0.025	0	0

chemical variations induced by weathering are characterized by an intense leaching of Na and F, as well as an important and progressive decalcification. These changes are accompanied by an increase of *A*- (Fig. 3) and *Y*-site deficiencies and by hydration, as is suggested by the sum of the analysed oxides (Table 2). The average H_2O content (calculated from 217 microprobe analysis) is 9.7±3.4%. The sum of cations occupying site *A* is between 0.02 and 0.65. The contents of the other elements present in the *B* site of the pyrochlores do not show significant variations.

The supergene alteration of pyrochlore is moving the data points towards the *VA* pole (Fig. 3; cation deficiency = 2), which corresponds to the extreme end member $\square_2Nb_2O_5\square_2H_2O$. This supergene tendency results in an almost complete leaching of Na and F through substitution (1) followed by a gradual loss of Ca essentially through substitution (2) (Nasraoui, 1996):

$$^{A}\mathrm{Na} + {}^{Y}\mathrm{F} = VA + VY \qquad (1)$$

$$^{A}\mathrm{Ca} + {}^{Y}\mathrm{O} = VA + VY \qquad (2)$$

Pyrochlores presenting significant leaching of the *A* site (*VA* near 2) have an oxygen value close to 5. This negative correlation between *VA* and oxygen (of the *X* site) can be explained by substitution (3) (*VX*: vacancies on the *X* site).

$$^{A}\mathrm{Ca} + {}^{X}\mathrm{O} = VA + VX \qquad (3)$$

These results corroborate the findings of Lumpkin and Ewing (1995) on the supergene alteration of pyrochlore in laterite from Araxa (Minas Gerais, Brazil).

The mineral species belonging to the pyrochlore sub-group and which are seen in the Lueshe laterite are kalipyrochlore, bariopyrochlore, strontiopyrochlore and a Na poor pyrochlore. All these minerals move away slightly from the extreme theoretical end-member $\square_2Nb_2O_5\square_2H_2O$ through partial filling of the *A* site via cationic exchange reactions (Nasraoui, 1996; Nasraoui and Bilal, 1997).

Results

Fourier transform infrared spectroscopy

The separated grains of weathered pyrochlore were porous and intensely fractured. The SEM observations show that they often present a continuous coating of crandallite and sometimes millisite. Subhedral to euhedral fresh pyrochlore grains are free of coatings, but they contain calcite inclusions. Figure 4 represents the IR absorbance spectra of fresh and weathered pyrochlore. The two spectra are very different.

An overview of the spectrum characterizing the weathered pyrochlore allows us to outline the most significant absorbance bands. It yields a large absorption band in the vibration zone of OH (stretching) between 3500 and 3200 cm^{-1} with a peak at ~3413 cm^{-1}, as well as a finer band of H–OH (bending) ~1630 cm^{-1}. A clear band at ~1041 cm^{-1} which may correspond to the stretching vibration mode of P–O is also visible, whereas the 884 cm^{-1} absorbance band may be attributed to the vibration of the HPO_4 grouping. These two bands confirm the presence of phosphate minerals, which corroborate the SEM observations (occurrence of crandallite and millisite). The band at 1041 cm^{-1} shows a

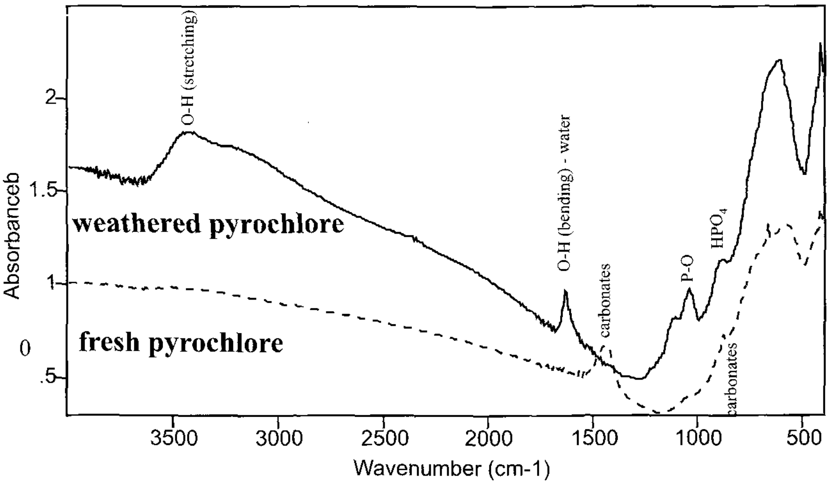

G. 4. IR absorbance spectra of fresh and weathered pyrochlore. The spectra represent an average of 32 scans, the resolution is 4 cm^{-1}.

shoulder at ~1110 cm^{-1}, which can be attributed, together with a large band at ~616 cm^{-1}, to the pyrochlore fundamental vibrations (Krivokoneva and Sidorenko, 1971).

Unlike the IR absorbance spectrum of the weathered pyrochlore, that of the fresh pyrochlore yields absorbance bands that are characteristic of the vibration modes of carbonate ions (Alder and Kerr, 1962; White, 1974). The peak at 1438 cm^{-1} represents the vibration of the double valence (v3) of the C–O grouping, whereas the peak at 876 cm^{-1} corresponds to the vibration v2 (out-of-plane bending) of CO_3. The SEM observations of fresh pyrochlore grains revealed the presence of solid inclusions of calcite. The large band characteristic of pyrochlore (575 cm^{-1}) is moved slightly towards the weaker wavelength (in comparison to that of the weathered pyrochlore), while the band at ~1110 cm^{-1} is hardly detectable.

Coupling of FTIR and thermal analysis

If the application of thermal analysis to geological materials, especially in mineralogical studies, is relatively common (Kulp *et al.*, 1952; Krivokoneva and Sidorenko, 1971; Mackenzie, 1972; Todor, 1976; Lindqvist and Rehtijärvi, 1979; Warne, 1987; Earnest, 1988; Stoch, 1991), the combination of thermal analysis and FTIR spectroscopy is rare. This combination is particularly interesting because it allows us to

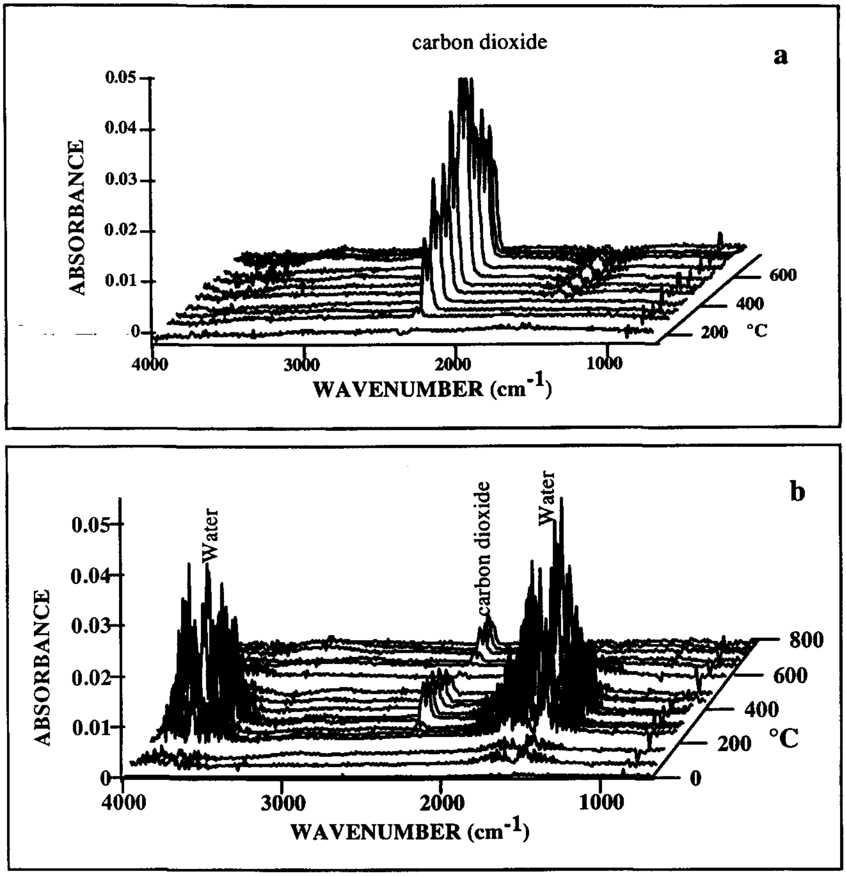

FIG. 5. 3D view of gas emission during temperature increase in the study of (*a*) fresh pyrochlore; and (*b*) weathered pyrochlore.

follow and to characterize the loss of masses during a specific thermal program, and to obtain a DSC curve.

Characterization of gas emanations during the thermal program

Fresh pyrochlore

The characterization of the emission gas during temperature increase provides interesting information about the structural modifications, the chemical reactions and other textural changes affecting the studied sample. This information often complements that obtained by DSC. The study of the fresh pyrochlore shows an emission of CO_2 during temperature increase (Fig. 5*a*). This CO_2 emanation begins ~242°C (12.44 min) and is maintained until 576°C (29.24 min). No gas emission is detected above these temperatures.

Weathered pyrochlore

The observation of the gas emanation during the thermal evolution of the weathered pyrochlore indicates a more complex composition of the sample. Water release and a biphased emission of CO_2 can be seen during the temperature increase (Fig. 5*b*). We also noticed that: (1) an initial release of water (probably adsorbed) occurs between 64 and 150°C (two small peaks after 3.9 min). (2) A release of water associated with the crystalline structure begins at ~234°C (after 12 min). (3) At ~296°C, the same time as the release of water, the first liberation phase of CO_2 occurs. It is later than that in the case of fresh pyrochlore. (4) This phase of CO_2 release is maintained up to temperatures of ~411°C (20.9 min). (5) The release of water is completed at ~565°C and the second phase of CO_2 release begins at 712°C up to 775°C (39.6 min).

Thermal analysis

The thermal analysis was conducted in inert conditions with Ar as the flowing gas. The neutral atmosphere prevents oxidation reactions which can interfere with the transformation of the pyrochlore during the increase of temperature. The DSC, TG (thermogravimetric analysis) curves, and its derivative (DTG) are presented. In order to compare the results of the thermal evolution of the fresh and the weathered pyrochlore, we operated under the same analytical conditions and on identical masses of sample. For the fresh pyrochlore, no significant enthalpy variation was observed, illustrating its high stability during increase of temperature. Other authors (Kulp *et al.*, 1952; Krivokoneva and Sidorenko, 1971; Lindqvist and Rehtijärvi, 1979) have reported this absence of reaction during

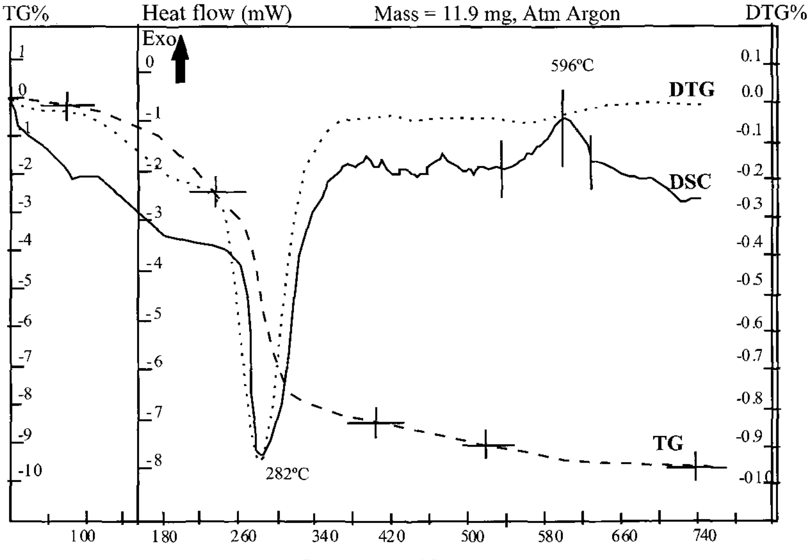

FIG. 6. DSC, TG and DTG curves of weathered pyrochlore.

thermal processing. Figure 6 presents the DSC, TG and DTG curves obtained on 11.9 mg of a weathered pyrochlore sample heated to 800°C (10°C/min). The first endothermic peak (DSC) at 76°C is correlated with a loss of 0.2% of the mass of the sample. It is induced by the release of adsorbed water, as shown in the IR gas analysis (Fig. 5*b*). The second endothermic peak (T_{max} = 282°C) is linked to the simultaneous release of water and CO_2 (first phase). The loss of the corresponding mass is close to 9% of the initial mass of the sample. A possible analogy exists between the variations in the DTG and DSC curves. An exothermic peak is observed at between 540 and 645°C, whose reproducibility was demonstrated by two linear programs of increasing temperature: the first with a temperature increase of 20°C/min, and the second, 10°C/min. A slight shift of the exothermic peak towards the high temperatures (604 instead of 596°C) was noticed during the faster rate of temperature increase (20°C/min). The sample powder was examined by XRD before and after heating in order to identify the mineralogical transformations. The whitish powder before heating became pinkish after heating. The exothermic peak could correspond to the crystallization of a niobium oxide. The XRD pattern of the sample before heating corresponds to that of a referenced hydrated bariopyrochlore (the lattice parameter a = 10.549) from Panda Hill (Tanzania), a small amount of crandallite also being detected. The XRD pattern of the sample after heating corresponds to that of the referenced pyrochlore heated to 700°C (the lattice parameter a = 10.366) from Oka carbonatite (Quebec, Canada) to which a new phase is added. This latter corresponds to a niobium oxide (Nasraoui, 1996).

Discussion

Infrared analysis (absorbance) allows a precise characterization of the mineral phases present in each sample. This mineralogical signature is very visible in the spectra (Fig. 4); caused by the occurrence of calcite in the fresh pyrochlore and aluminous phosphate in the weathered pyrochlore. The important hydration state of the weathered pyrochlore is remarkable, outlined by the presence of the intense bands of OH at 3413 cm^{-1} (stretching) and 1630 cm^{-1} (bending). This hydration explains, to a large extent, the low sum of the microprobe analysis of the weathered pyrochlore.

Thermal analysis results also allow a precise evaluation of the structural stability of the pyrochlore according to its alteration state. The fresh pyrochlore does not show any transformation during the increase in temperature. The only detectable change is the emanation of CO_2 between 242 and 576°C, which may be related to a decomposition of calcite inclusions. The weathered pyrochlore is differentiated from fresh pyrochlore by its structural fragility, leading to mineralogical transformations during the thermal processing. After a release of adsorbed water (from 64–150°C), the thermal evolution of weathered pyrochlore is marked by a dehydration between 234 and 565°C. It is also accompanied by a loss of mass of ~9% and by a decrease in the lattice parameter a. This dehydration is followed by a crystallization of a new orthorhombic phase (a = 6.175 Å, b = 29.175 Å, c = 3.930 Å) of niobium oxide. This phase is shown by an exothermic peak in the DSC curve in a temperature interval of 540 to 640°C, the maximum of the peak occurring at 594°C. The formation temperature of the Nb_2O_5 phase is closely linked to dehydration of the weathered pyrochlore. Weathering processes change the pyrochlore from a primary composition close to the ideal formula $(Ca,Na)_2Nb_2O_6F$ to a deficient hydrated end-member of the type $\square_2Nb_2O_5\square_1 2H_2O$ and its variants (bariopyrochlore: $Ba_\varepsilon Nb_2O_{5+\varepsilon}2H_2O$, strontiopyrochlore: $Sr_\varepsilon Nb_2O_{5+\varepsilon}2H_2O$ and kalipyrochlore: $K_{2\varepsilon}Nb_2O_{5+\varepsilon}2H_2O$), by the substitutions (1) and (2). In response to the increase in temperature, the dehydration of the weathered pyrochlore can begin when the energy generated is greater than that binding the water to the structure. When this dehydration is complete, the structure of the pyrochlore is destabilized and crystallization of the orthorhombic phase of niobium oxide (Nb_2O_5) may occur. Some thermal analysis studies, carried out on metamict pyrochlore, have shown that the formation of new phases is closely dependent on the initial composition of the pyrochlore. When it contains Ca, fersmite can appear during the 750–930°C temperature interval (Gorzhevskaya and Sidorenko, 1962), whereas lueshite originates from fresh pyrochlore and seems to be favoured by an active atmosphere (Gorzhevskaya and Sidorenko, 1962; Lindqvist and Rhehtijärvi, 1979). In summary, water plays an essential role in the stability of the weathered pyrochlore and consequently in the sensitivity of this mineral to further changes, especially when the temperature increases.

The biphased emanation of CO_2 could be linked to the presence of crandallite and millisite in the original sample. These two minerals could contain CO_3^{2-} in their structures as substitutes of PO_4^{3-}, and they are potentially able to release CO_2 during the heating program. The amounts of crandallite and millisite in the studied sample are very small. The precise characterization of the departures of CO_2 is due to the high sensitivity of the method. According to the Beer law ($A = \varepsilon_\lambda lc$), in which absorbance A of a gas is linked to its concentration c (mol l^{-1}), to the length l (cm) of the gas tube and to a specific coefficient ε_λ of the gas, this coefficient is very large in the case of CO_2. Consequently it magnifies the absorbance peak of this gas and prohibits all quantitative comparison between the emanation of different gas (without preliminary calibration).

Conclusions

The combination of FTIR spectroscopy with thermal analysis provides much information which cannot be obtained by the classical microanalytical methods. The hydration which takes place during the weathering processes of pyrochlore, normally detected by microprobe analysis, is well detected by IR.

The study of the thermal evolution of pyrochlores by coupling FTIR and thermal analysis shows two sets of contrasting behaviour among weathered and fresh pyrochlore. The latter shows a high structural stability during the thermal program, whereas the weathered pyrochlore is more vulnerable. This vulnerability is shown in the DSC curve by an exothermic peak denoting a mineralogical change which is closely related to the completion of the dehydration of the mineral. This is a strong argument in favour of the stabilizing role of water in the structure of weathered pyrochlore. Processing of weathered pyrochlore by heating could be used for the enrichment of Nb especially in the low Nb grade ores.

The combination of FTIR with thermal analysis is a powerful technique if the textural and mineralogical parameters of the studied material are taken into account.

Acknowledgements

The authors are very grateful to Norbert Clauer, Terry Williams and two anonymous reviewers for useful comments which have much improved the manuscript. This study was supported by the European Community (EEC contract no. MA2M CT90 0038).

References

Albers, K.H., Alegria, B., Meixner, K.-T., Schuermann, B., Phillipo, S., Naud, J., Verkaeren, J., Nasraoui, M., Bilal, E., Garcia, D., Gruffat, J.J., Guy, B., Moutte, J., Wall, F., Williams, C.T. and Woolley, A.R. (1994) *Applied mineralogy of pyrochlore and related minerals in the weathering zones of the niobium deposits of the Lueshe and Bingo carbonatites, Zaire. Final Report to European Commission. EC Contract No: MA2M-CT90-0038. Unpublished.* 138 pp.

Alder, H.H. and Kerr, P.F. (1962) Infrared study of aragonite and calcite. *Amer. Mineral.*, **47**, 700–11.

Bellon, H. and Pouclet, A. (1980) Datations K/Ar de quelques laves du Rift-Ouest de l'Afrique Centrale; implication sur l'évolution magmatique et structurale. *Geol. Runds.*, **69**, 49–62.

De Bethune, P. (1949) Sur les manifestations bénignes du métamorphisme. *Acad. Roy. Belg. Bull. Classe des Sciences*, **5(t35)**, 1073–88.

De Bethune, P. (1952) Etudes pétrographiques dans les monts Rwindi (Kivu, Congo Belge). *Mém. hist. Géol. Univ. Louvain*, **16**, 221–9.

Earnest, C.M. (1988) Compositional analysis by thermogravimetry. *ASTM Spec Tech Publ.*, **997**, Philadelphia.

Ercit, T.S., Hawthorne, F.C. and Černý, P. (1994) The structural chemistry of kalipyrochlore, a 'hydropyrochlore'. *Canad. Mineral.*, **32**, 415–20.

Gorzhevskaya, S.A and Sidorenko, G.A. (1962) Phases obtained by heating minerals with pyrochlore structure and the relation of these phases to the chemical composition of the original minerals. *Geokhimiya*, **9**, 794–9.

Hogarth, D.D. (1977) Classification and nomenclature of the pyrochlore group. *Amer. Mineral.*, **62**, 403–10.

Hogarth, D.D. (1989) Pyrochlore, apatite and amphibole: distinctive minerals in carbonatite. In *Carbonatites: Genesis and Evolution* (K. Bell, ed.). Unwin Hyman, London, 105–48.

Krivokoneva, G.K. and Sidorenko, G.A. (1971) The essence of the metamict transformation in pyrochlores. *Geochem. Int.*, **8**, 113–22.

Kulp, J.L., Volchok, H.L and Holland, H.D. (1952) Age from metamict minerals. *Amer. Mineral.*, **37**, 709–18.

Lindqvist, K. and Rehtijärvi, P. (1979) Pyrochlore from the Sokli carbonatite complex, Northern Finland. *Bull. Geol. Soc. Finland*, **51**, 81–93.

Lubala, R.T, Kampunzu, A.B. and Makutu, M.N. (1985)

Un inventaire des complexes anorogeniques du Burundi, du Rwanda et du Zaïre. *J. African Earth Sci,*. **3(1/2)**, 169–74.

Lumpkin, G.R. (1989) *Alpha-decay damage, geochemical alteration, and crystal chemistry of pyrochlore group minerals*. Ph.D. thesis, University of New Mexico, Albuquerque.

Lumpkin, G.R and Ewing, R.C. (1995) Geochemical alteration of pyrochlore group minerals: Pyrochlore subgroup. *Amer. Mineral.*, **80,** 732–43.

Lumpkin, G.R., Chakoumakos, B.C and Ewing, R.C. (1986) Mineralogy and radiation effects of microlite from the Harding pegmatite, Taos County, New Mexico. *Amer. Mineral.*, **71**, 569–88.

Mackenzie, R.C. (1972) *Differential thermal analysis, Vol. 1. Fundamental aspects and Vol. 2 Applications*. Academic Press, New York.

Maravic, H.V. and Morteani, G. (1980) Petrology and geochemistry of the carbonatite and syenite complex of Lueshe (N.E. Zaïre). *Lithos.*, **13**, 159–70.

Maravic, H.V., Morteani, G. and Roethe, G. (1989) The cancrinite-syenite/carbonatite complex of Lueshe, Kivu, NE-Zaïre: petrographic and geochemical studies and its economic significance. *J. African Earth Sci.*, **9(2)**, 341–55.

Meyer, A. (1958) La carbonatite de Lueshe (Kivu). *Congo Belge, 4e Direction Générale, Service Géologique*, Bulletin n° 8-Fasc. 5. 8 pp.

Nasraoui, M. (1996) *Le gisement de niobium de Lueshe (Nord Est du Zaïre): Evolutions géochimique et minéralogique d'un complexe carbonatitique en contextes hydrothermal et supergène*. Ph.D. thesis, Geology and Mining Research, Ecole des Mines de Paris/ Ecole des Mines de Saint Etienne, 256 pp.

Nasraoui, M. and Bilal, E. (1997) Pyrochlore from Lueshe carbonatite: a geochemistry memory of different alteration stages. (in prep.)

Phillipo, S. (1995) *Evaluation minéralogique par diffraction des rayons X qualitative et quantitative des gisements latéritiques de niobium de la Lueshe et de Bingo dans le cadre de l'optimisation de la récupération du pyrochlore*. Ph.D. thesis, Université Catholique de Louvain, 207 pp.

Stoch, L. (1991) Internal thermal reactions of minerals. In *Thermal Analysis in the Geosciences*. (W. Smykatz-Kloss and S.St.J. Warne, eds.) Springer-Verlag Vol. **38**, 118–33.

Todor, D.N. (1976) *Thermal Analysis of Minerals*. Abacus Press, Tunbridge Wells, UK.

Van Overbeke, A.C. (1996) *Le complexe à carbonatite et syénite de Lueshe (N. Kivu, Zaïre): pétrogenèse des roches ignées et caractérisation géochimique des processus métasomatiques (fénitisation)*. Ph.D. thesis, Université Catholique de Louvain, 235 pp.

Van Wambeke, L. (1978) Kalipyrochlore, a new mineral of the pyrochlore group. *Amer. Mineral.*, **63**, 528–30.

Wall, F., Williams, C.T., Woolley, A.R. and Nasraoui, M. (1996) Pyrochlore from weathered carbonatite at Lueshe, Zaire. *Mineral. Mag.*, **60**, 731–50.

Warne, S.St.J. (1987) Applications of thermal analysis to carbonate mineralogy. *Thermochim. Acta*, **110**, 501–11.

White, W.B. (1974) The Carbonate Minerals. In *The Infrared Spectra of Minerals*, (V.C. Farmer, ed.), Mineralogical Society Monograph **4**, 227–84.

[*Manuscript received 12 January 1997:*
revised 20 July 1998]